Received: 8 September 2017 | Revised: 7 June 2018 | Accepted: 20 June 2018
DOI: 10.1002/acs.2915

RESEARCH ARTICLE

WILEY

Early malfunction diagnosis of industrial process units utilizing online linear trend profiles and real-time classification

T. Vafeiadis[1] | C. Ziogou[2] | G. Stavropoulos[1,3] | S. Krinidis[1] | D. Ioannidis[1] | S. Voutetakis[2] | D. Tzovaras[1] | K. Moustakas[3]

[1]Information Technologies Institute, Centre for Research & Technology Hellas, Thermi, Greece

[2]Chemical Process and Energy Resources Institute, Centre for Research & Technology Hellas, Thermi, Greece

[3]Department of Electrical and Computer Engineering, University of Patras, Patras, Greece

Correspondence
T. Vafeiadis, Information Technologies Institute, Centre for Research & Technology Hellas, 570 01 Thermi, Greece.
Email: thanvaf@iti.gr

Funding information
European Commission through the Horizon 2020 Framework Programme, Grant/Award Number: 636302

Summary

The early detection of potential malfunctions at process systems can significantly reduce downtime and improve their overall operability. In that context, this paper demonstrates the behavior and response, through a comparative analysis, of novel data-driven diagnosis methods for interdependent time series. The proposed real-time slope statistic profile method utilizes a self-adaptive sliding window based on a real-time classification technique of linear trend profiles of both interdependent time series and internal condition so as to avoid misdetections. The calculation of the linear trend profile is based on a standard parametric linear trend test, and the selection of possible incidents is based on its two-level cross-checking. All possible combinations for the calculation of the trend test and cross-checking are created to explore their efficiency. The proposed methods are tested against real data sets from a chemical process system of the Centre for Research and Technology Hellas/Chemical Process Energy and Resources Institute derived from specific scenarios during nominal operating conditions.

KEYWORDS

classification, early malfunction diagnosis, linear trend, structural change, time series

1 | INTRODUCTION

During the last decades, the term incident detection (or anomaly detection) in scientific literature refers to a problem of finding patterns in data that do not conform to expected normal behavior. The importance of incident detection is attributed to the fact that incidents in data translate to significant (and often critical) actionable information. Most of the existing incident detection techniques confront only specific areas of a problem with different techniques, according to their application domain and not in a generic form. In the literature, one can find many approaches on incident detection, such as artificial intelligence, classification,[1-5] the clustering approach,[6] and the statistical approach.[7,8] The artificial intelligence techniques applied in incident detection problems include neural networks (backpropagation, support vector machines, and decision trees), fuzzy logic, and a combination of these two techniques.[9]

In time series analysis, incident detection is referred to as structural change. In the past years, the problem of structural change(s) detection in time series has received a great deal of attention in areas such as meteorology and earth sciences,[10,11] communication and social networks,[1,12,13] applied economics,[14,15] urban data,[16] and chemical process,[17] among others.

Recently, incident detection has been an important and difficult issue of increasing interest also in econometrics and statistics literature.[18,19] Time series algorithms assume that the imported data normally follow a predictable pattern over time, and they use time series models to predict normal conditions and detect incidents when imported measurements deviate significantly from model outputs. Furthermore, in most of the aforementioned cases, a single-variable analysis is performed where the incidents are related to a single time series, ignoring the effect that other variables might have by potential interactions. This work examines that case of incident detection between two independent time series.

Overall, incident detection algorithms and methods may be grouped into two categories: automatic and nonautomatic. Automatic algorithms are those that automatically trigger an incident alarm when data are received from a field of sensors that satisfy certain predefined conditions. On the contrary, nonautomatic algorithms are those that are based on the worker's reports and experience. A number of studies can be found that contain interesting comparisons between methods and evaluations of algorithms for incident detection.[20-25] It has to be mentioned that all of the aforementioned algorithms and techniques are applied or modified in order to cover specific incident detection use cases.

Early malfunction detection is an important area in process engineering that deals with the timely detection and diagnosis of abnormal conditions of incidents (faults) in a process.[26] The early notification and detection of a process malfunction or a potential malfunction while the plant is in operating mode and in a controllable region can significantly prevent abnormal and potentially unsafe event progression and reduce productivity loss. The malfunctions are related to faults, which are defined as the deviation from an acceptable range of an observed variable or a calculated parameter related to a process.[27] In this work, the incident detection problem is considered in the context of monitoring of chemical process systems using time series related to critical areas, such as a chemical reactor. More specifically, the time series corresponds to the behavior of a heating zone where a temperature controller maintains the temperature of the external zone to the desired set point as defined by the operating conditions for each experiment. The heating zones are part of a chemical process pilot plant that is designed, constructed, and operated by the *Centre for Research and Technology Hellas/Chemical Process Energy and Resources Institute* (CERTH/CPERI). In our case, all detected incidents denote a potential malfunction of the heating zone. This work is essentially an extension of the works of Vafeiadis et al[28,29] on the utilization of the modified versions of the slope statistic profile, denoted hereafter as SSP, methodology on two interdependent time series produced at the same time and provides two more modified versions along with a final comparison among them.

The novelty of this comparative work is that it provides the ability to infer the presence of an incident in real time soon after the incident actually occurs (early malfunction diagnosis) of industrial time series based on the simultaneous calculation and analysis of linear trend profiles of two interdependent time series, utilizing an overlapping sliding data window. Early malfunction diagnosis is achieved with the use of a modified approach of the SSP for real-time estimation, with its basic feature being the ability to resize autonomously the size of the sliding window (utilizing real-time classification) based on the information acquired in real time from the linear trend profiles of the interdependent time series.

This paper is organized as follows. In Section 2, the incident detection problem is defined. A brief description of the existing versions of the real-time slope statistic profile, denoted hereafter as RTSSP, method is given in Section 3, whereas the novel development of a self-adaptive sliding window and a common point condition (CPC) are given in Section 4. In Section 5, a comparison is performed between the existing and newly developed versions of the RTSSP method, and in Section 6, we draw our conclusions.

2 | PROBLEM DEFINITION AND INCIDENT/MALFUNCTION DETECTION

In general, the categories of failures or malfunctions at a process can be originated by sensor failures, actuator failures, or a controller malfunction.[26] Although a number of different cases exist that can be used to derive the root cause of a problem, in this work, the focus is toward the analysis of the response of control loops and, more specifically, temperature control loops. In order to develop and test an early malfunction diagnosis mechanism, a pilot case is selected that deals with two interdependent time series, which is a fact that reacts positively not only to the development of a modified approach of the SSP but also to the autonomous decision of the sliding window size through a novel technique. The time series are from the operation of a chemical process of CERTH/CPERI. The experimental data are gathered online and are acquired by the local industrial automation system infrastructure, in order to be used for comparative analysis during this work. More specifically, the behavior of a heating zone of a reactor is studied. The objective is to be able to detect as soon as possible a potential malfunction while the reactor is in operation. The temperature conditions of the reactor are maintained by a set of heating zones and are affected by the dynamically evolving exothermic or endothermic reactions

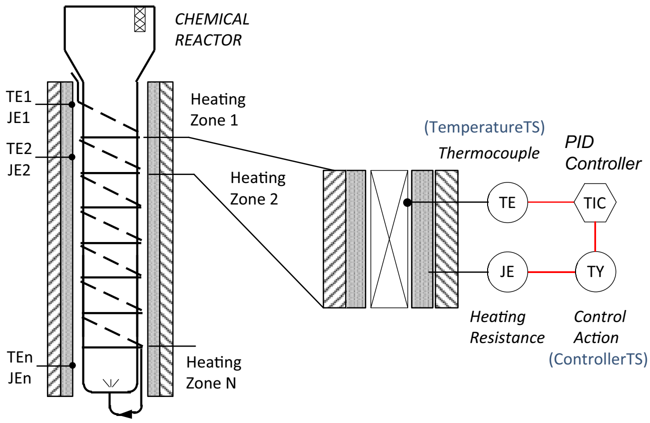

FIGURE 1 The components of a typical heating zone of a chemical reactor. PID, proportional integral derivative; JE, heating resistance; TE, thermocouple; TIC, controller; TY, solid-state relay

that take place during the reactor operation. Figure 1 shows the typical structure of a chemical reactor with heating zones along with the analysis of the active measurement and control elements of an indicative heating zone. These elements are the thermocouple (TE) that measures the temperature, the controller (TIC) that calculated the appropriate action to reach or maintain the desired temperature, the solid-state relay (TY) that implements the control action received by the controller, and the heating resistance (JE).

For each heating zone, there is a measured input variable, ie, the temperature (hereafter denoted as TemperatureTS), and an output variable, ie, the percentage of operation of the heating resistance. In order to maintain the heating zone to a desired temperature set point, a controller is used (hereafter denoted as ControllerTS) that defines the percentage of operation (0%-100%) of the heating resistance according to the measured temperature. A proportional-integral-derivative controller is used as a control loop feedback mechanism that continuously calculates an error value as the difference between the measured temperature and the desired set point. The controller attempts to minimize the error over time by the adjustment of the control variable, which is the power supplied to the heating element. These two signals constitute the tuple of the time series that will be fed to the proposed method. Overall, the relationship of these interdependent time series is that when one decreases (TemperatureTS), the other increases (ControllerTS) (see Figure 1) when the set point is higher than the measured temperature, and vice versa. In case the temperature steadily decreases while the controller output increases, this indicates that a potential malfunction might be present, which can be attributed to various reasons such as the short circuit of the heating resistance or a burned fuse at the electrical cabinet. When an incident like this occurs, the operation of the process unit needs to stop for maintenance actions to take place and restore the fault. Overall, this type of downtime can affect not only the evolution of a single experiment but also the overall unit as it needs to reach a shutdown state where its temperature is close to environmental conditions and after the fault correction to be heated up again to reach the appropriate temperature conditions. The entire procedure is translated into wasted time, material, and resources.

The interdependency of both time series is also verified by Pearson's correlation, where the calculated correlation shows that TemperatureTS and ControllerTS are highly anticorrelated time series when an incident occurs.[29] Thus, the case where TemperatureTS output decreases while ControllerTS output increases indicates that a malfunction might be present. The incident that the proposed method will target to detect is the aforementioned case. Figure 2 shows two data sets, namely, DS1 (Figure 2A) and DS2 (Figure 2B), which represent the controller output and the temperature during a 24-hour period used for the comparison and evaluation of all modified versions of the SSP. The data sets are from different heating zones from a continuous chemical process unit of pilot scale, which is used for the evaluation of chemical catalysts. These indicative data sets are selected because they present two different scenarios of failure, with different responses of the temperature profile. Despite the difference on failure scenarios, one can see the steady state of the controller and temperature time series, in the interval of [0, 580] minutes in Figure 2A and in the interval of [0, 130] minutes in Figure 2B. This steady-state form is similar to all tested data sets.

It can be seen that the operating temperature is different between the two cases. In the first case (DS1), the temperature reaches a new steady-state level after the malfunction as it is affected by its adjacent heating zones; thus, it takes longer to lose its heat compared to the case of DS2, where it is observed that a rapid decrease in temperature occurs.

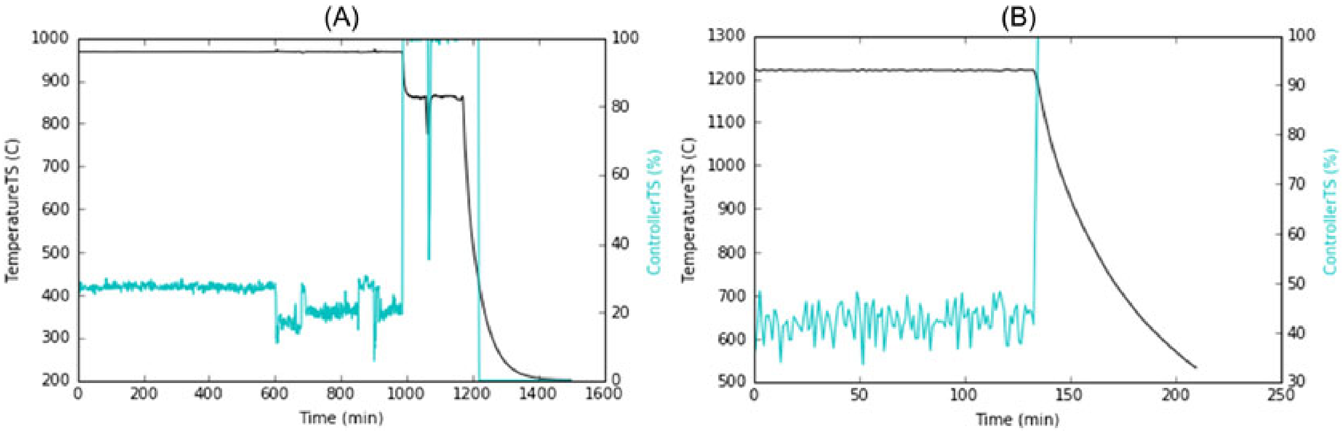

FIGURE 2 TemperatureTS (black solid line) and ControllerTS (cyan solid line) time series during an experiment of the chemical reactor in the premises of the Centre for Research and Technology Hellas/Chemical Process Energy and Resources Institute when an incident occurs. Tested data sets are (A) DS1 and (B) DS2

3 | MODIFIED SSP FOR REAL-TIME INCIDENT DETECTION

An SSP method for real-time incident detection, based on real-time classification of linear trend profiles, has been previously studied, targeting an automatic and parameter-free approach so as to provide more accurate and significant incident detections.[28,29] This work extends the aforementioned method to a more comprehensive and integrated approach. A brief description of the modified versions of the SSP method is given.

The SSP method estimates the change point (or breakpoint T) of the linear trend in a time series from the profile of a linear trend test statistic, computed on consecutive overlapping sliding data windows along the time series. The sliding window is a technique that processes the most recent data points of the time series and moves s steps along the time axis as new measurements arrive. This technique has the advantage that it does not need to store the never-ending data stream of data. Also, it implies that only the measurements located within the current window can be considered for further data analysis. The selected sliding window step is one, so as not to lose any information regarding changes in the linear trend of the tested time series. In this work, we adapt two test statistics for linear trend estimation that gives high test power: one for the correlated residual and another for both correlated and white noise residuals.[27] In the SSP approach, a first candidate breakpoint T is the time point at which the calculated linear trend profile t_c crosses the threshold line of rejection of the null hypothesis of no trend at $\pm t_{w-2,1-\frac{a}{2}}$, where a is the significance level, w is the size of the sliding window, and t_c follows the Student distribution with $w - 2$ degrees of freedom ($t_c \sim t_{w-2}$).[30] The search of the change point is confined in a time interval corresponding to the profile segment bounded by $t_{w-2,1-a_1/2}$ and $t_{w-2,1-a_2/2}$ for positive trends and by $-t_{t_{w-2,1-a_2/2}}$ and $-t_{w-2,1-a_1/2}$ for negative trends, where the significance levels a_1 and a_2 for the two-side test are 0.20 and 0.05, respectively.[7] The selection of two significant levels is based on the assumption that there are not sudden and abrupt changes in natural variations, which means that more time and information is needed for a time series to pass from a zero trend to trend status, and vice versa. Thus, the existence of two significant levels describes the transition between these situations. Hereafter, segment $(t_{w-2,1-a_1/2}, t_{w-2,1-a_2/2})$ will be denoted as the upper-bound (UB) segment and $t_{w-2,1-a_1/2}$, $t_{w-2,1-a_2/2}$ as UB_1 and UB_2, respectively, and segment $(-t_{w-2,1-a_2/2}, -t_{w-2,1-a_1/2})$ will be denoted as the lower-bound (LB) segment and $-t_{w-2,1-a_1/2}$, $-t_{w-2,1-a_2/2}$ as LB_1 and LB_2, respectively. The computational study by Vafeiadis et al[7] showed that in case of a time series of known size, the sliding window should be long enough (larger than 30% of the time series length), so that the estimation of other spurious onsets occurring at small time scales is avoided. In real time, the size of the sliding window is self-adapted as proposed in the works of Vafeiadis et al.[28,29]

At this point, a brief description of the linear trend test statistic that is used in the SSP method is given. In the following, the parametric linear trend test for a sliding window of size w on the time series Y_t, $t = 1, \ldots, n$, is presented. Thus, for the first window $[\mathrm{Y}_1, \ldots, \mathrm{Y}_w]^T$, the least squares estimator for the trend parameter β is obtained as

$$\hat{\beta} = \frac{\sum_{t=1}^{w}(t-\bar{t})Y_t}{\sum_{t=1}^{w}(t-\bar{t})^2}, \tag{1}$$

where $\bar{t}$ is the average time. The standard error of $\hat{\beta}$ can be estimated with several approaches. Here, the best two approaches are presented: the autocovariance and the power spectrum approach. In the autocovariance approach, under the assumption of independent and normally distributed residuals ε_t with zero mean and variance σ^2, the estimated standard error of $\hat{\beta}$ is calculated by

$$s_1(\hat{\beta}) = \left\{ c \left[\gamma_0 + 2c \sum_{s=2}^{w} \sum_{t=1}^{s-1} (t-\bar{t})(s-\bar{t})\gamma_{s-t} \right] \right\}^{1/2}, \tag{2}$$

where $c = \frac{12}{w(w^2-1)}$. The estimated residuals are given by $\hat{\varepsilon}_t = Y_t - \hat{\alpha} - \hat{\beta}t$, where $\hat{\alpha} = \overline{Y_t} - \hat{\beta}t$ and $\overline{Y_t}$ is the average of the time series. In (2), γ_k is replaced with the respective estimate of $\hat{\gamma}_\kappa$, except at $k = 0$ where $w\hat{\gamma}_0/(w-2)$ is used in order to estimate γ_0.[30] Thus, the estimated standard error of $\hat{\beta}, s_1(\hat{\beta})$ is derived. In the power spectrum approach, the estimated standard error of $\hat{\beta}$ is calculated by

$$s_2(\hat{\beta}) = \left[2 \int_0^{0.5} W(f)S(f) \right]^{1/2}, \tag{3}$$

where $W(f) = \left| \sum_{t=1}^{w} b_t e^{-2\pi i f} \right|^2$ with $b_t = \frac{t-\bar{t}}{\sum_{t=1}^{w}(t-\bar{t})^2}$ and $S(f)$ denotes the sample power spectrum of ε_t given as $S(f) = \frac{1}{2\pi}(\hat{\gamma}_0 + 2\sum_{\kappa=1}^{w-1} \hat{\gamma}_\kappa \cos(2\pi f k))$. $\hat{\gamma}_\kappa$ denotes the estimate of the kth-order autocovariance of ε_t, given as $\hat{\gamma}_\kappa = \frac{1}{w}\sum_{t=1}^{w-k} \hat{\varepsilon}_{t+k}\hat{\varepsilon}_t$ for $k > 0$ and $\hat{\gamma}_0 = \frac{1}{w-2}\sum_{t=1}^{w} \hat{\varepsilon}_t^2$ for $k = 0$. Thus, the estimated standard error of $\hat{\beta}, s_2(\hat{\beta})$ is derived.

The t-statistic for the parametric linear trend test is $t_{cm} = \frac{\hat{\beta}}{s_m(\hat{\beta})}$, where $m = 1$ is the autocovariance approach and $m = 2$ is the power spectrum approach. Both approaches of standard error estimation have different characteristics that affect the t-statistic. The autocovariance approach is more sensitive to small changes in the linear trend, and that makes the $t_{c1} = \frac{\hat{\hat{\beta}}}{s_1(\hat{\beta})}$ test statistic more condescending while the power spectrum approach gives high test power to test statistic $t_{c2} = \frac{\hat{\beta}}{s_2(\hat{\beta})}$ compared to other tests for both correlated and white noise residuals.

The SSP method is initially proposed for the time series of known size, and the crucial parameter of sliding window size is decided according to this time series size. However, in cases where the SSP method has to apply in real time, the original version is not practical due to the fact that the selection of the proper size of the sliding window is a challenging decision, since the form of ControllerTS and TemperatureTS varies. The solution that Vafeiadis et al have proposed[28] is the RTSSP, which addresses the issue of the sliding window size selection, among others.

Two different versions of the RTSSP method have been developed based on the computation of the standard error of the linear trend parameter and the setup of segments. Both versions have embedded a real-time classification technique for the decision of the sliding window size to be automatic and self-adaptive. As mentioned above, t_c is computed on overlapping data windows of size w with sliding step one. Thus, the RTSSP curve ($\{RTSSP_i\}$ for $i = w, w+1, w+2, \ldots$) for the entire time series created so far is obtained. In the first version, denoted hereafter as RTSSPv1, the computation of the standard error estimator of the trend parameter is $s_1(\hat{\beta})$, and the possible incidents T are detected when the linear trend profiles of the selected time series cross only UB_1 and LB_1.[28] In the second version, denoted hereafter as RTSSPv2, the computation of the standard error estimator of the trend parameter is $s_2(\hat{\beta})$, and the possible incidents T are detected strictly inside the upper and lower segments.[29]

4 | SELF-ADAPTIVE SLIDING WINDOW—CPC

Despite the standard error calculation of the trend parameter and the different approaches in the cross-checking of linear trend profiles, both versions RTSSPv1 and RTSSPv2 use real-time classification techniques for the automatic adaptation of the size of the sliding window and a condition for the proper detection of incidents. Thus, the sliding window has the ability to dynamically change its size, between predefined minimum and maximum limits, for a better online monitoring process.

Linear trend profiles $\{RTSSP_i\}$ are both calculated for time series and classified in real time according to two different linear trend scenarios, suitably adjusted to the problem of estimation of abnormal temperature behavior incidents. Scenario 1 presents the case where the ControllerTS output time series moves in the fields of no trend and negative trend and the expectation of TemperatureTS time series to move in the fields of no trend and positive trend, respectively.

TABLE 1 Confusion matrices for Scenarios 1 and 2 of the linear trend profiles $\{RTSSP_i\}$ of ControllerTS and TemperatureTS for versions RTSSPv1 (a, b) and RTSSPv2 (c, d)

(a) Scenario 1 (Negative Trend for ControllerTS)		TemperatureTS $\{RTSSP_i\}$ $t_c \in (LB_1, UB_1)$	$t_c > UB_1$	(b) Scenario 2 (Positive Trend for ControllerTS)		TemperatureTS $\{RTSSP_i\}$ $t_c \in (LB_1, UB_1)$	$t_c < LB_1$
ControllerTS	$t_c \in (LB_1, UB_1)$	TP	FN	ControllerTS	$t_c \in (LB_1, UB_1)$	TP	FN
$\{RTSSP_i\}$	$t_c < LB_1$	FP	TN	$\{RTSSP_i\}$	$t_c > UB_1$	FP	TN
(c) Scenario 1 (Negative Trend for ControllerTS)		**TemperatureTS $\{RTSSP_i\}$ $t_c \in (LB_1, UB_1)$**	**$t_c \in (UB_1, UB_2)$**	**(d) Scenario 2 (Positive Trend for ControllerTS)**		**TemperatureTS $\{RTSSP_i\}$ $t_c \in (LB_1, UB_1)$**	**$t_c \in (UB_1, UB_2)$**
ControllerTS	$t_c \in (LB_1, UB_1)$	TP	FN	ControllerTS	$t_c \in (LB_1, UB_1)$	TP	FN
$\{RTSSP_i\}$	$t_c \in (LB_2, LB_1)$	FP	TN	$\{RTSSP_i\}$	$t_c \in (UB_1, UB_2)$	FP	TN

Abbreviations: FN, false negative; FP, false positive; LB, lower bound; RTSSP, real-time slope statistic profile; TN, true negative; TP, true positive; UB, upper bound.

TABLE 2 Intervals for FM1 and FM2 in which the sliding window size increases or decreases by C or remains steady

Conditions	Sliding Window w
$FM_1, FM_2 \in [FMB, FMB + 3\%)$	Steady
$FM_1, FM_2 \geq FMB + 3\%$	Decrease by c
$FM_1, FM_2 < FMB$	Increase by c

Abbreviations: FM, F-measure; FMB, F-measure bound.

On the other hand, Scenario 2 presents the exact opposite scenario compared to Scenario 1, with ControllerTS series to move in the fields on no trend and positive trend and the expectation of TemperatureTS time series to move in the fields of no trend and negative trend, respectively. In (a) and (b) of Table 1, the confusion matrices are given for Scenarios 1 and 2 of version RTSSPv1, whereas (c) and (d) of Table 1 give the confusion matrices for Scenarios 1 and 2 of version RTSSPv2, respectively.

The measures of precision, recall, accuracy, and F-measure are calculated from the context of the confusion matrix, shown in Table 1. True positive and false positive cases are denoted as TP and FP, respectively, whereas true negative and false negative cases are denoted as TN and FN. The instances of the confusion matrices shown in Table 1 are set in order to include both cases of positive and negative linear trends. Precision and recall cannot describe the efficiency of the method for selected parameters since a good performance in one of those indices does not necessarily imply a good performance in the other. For this reason, the F-measure (FM), a popular combination of precision and recall, is commonly used as a single metric for performance evaluation. The F-measure is defined as the harmonic mean of precision and recall.

Subsequently and despite the version of RTSSP, the size of w is calculated according to the real-time computed F-measure values of Scenarios 1 and 2, hereafter denoted as FM1 and FM2. The size of w will be changed by c time elements as follows: let us assume the existence of a bound in the F-measure value (FMB as percent). The existence of this bound aims firstly to test the effectiveness of the RTSSP method in extreme conditions of accuracy and secondly to provide a bound for the self-adaptation of the sliding window size. Table 2 explains the values of the adaptive window, based on the calculated F-measures and FMB. The value FMB + 3% is the allowed range where the sliding window changes. The +3% limit of the FMB values for the sliding window to be changed is selected after a series of simulations performed for several limits ranging from 3% to 10%, based on simulations performed for FMB (see Vafeiadis et al[28,29]). The minimum and maximum values of the sliding window size need to be preset.

Furthermore, since the classification of the linear trend profiles of both time series is performed online, the adaptation of the sliding window size is performed in real time, repeatedly every 100 time points. From the exhaustive simulations made in the works of Vafeiadis et al[28,29] for all internal parameters (sliding window size, F-measure bound, sliding window change, and maximum sliding window), simulation results show that the size of FMB can be set at 95% and the parameter of change of the sliding window can be set at $c = 20$ elements. As for the minimum and maximum values of sliding window size, those can be set to 40 and 120 elements, respectively. For all comparison tests that follow, the core values of methods' parameters are predefined according to prior simulation results and are indicative. On the other hand, the end user is allowed to experiment on parameter combinations in order to achieve the desired performance of the method on early malfunction diagnosis.

For both versions RTSSPv1 and RTSSPv2, potential incidents in the ControllerTS and TemperatureTS time series are chosen to be all the time points that are placed outside the UB_1 or LB_1 threshold or that are placed in the lower or upper

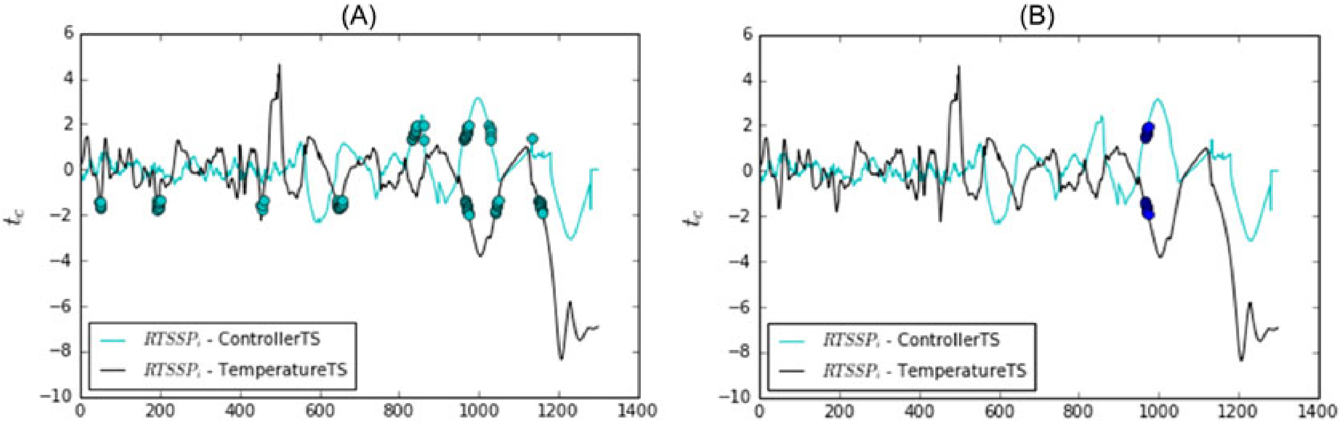

FIGURE 3 (A) Linear trend profiles $\{RTSSP_i\}$ of the ControllerTS and TemperatureTS time series and possible incidents T. (B) Detected incidents T after the application of a common point condition. RTSSP, real-time slope statistic profile

segments. This approach of the incident detection problem can result sometimes in the detection of too many incidents during the process ($\{RTSSP_i\}$ profiles of ControllerTS and TemperatureTS cross thresholds many times asynchronously), either on ControllerTS or TemperatureTS time series or for both of them. Thus, in order to avoid the misdetection of incidents (some of them may have no meaning at all), we impose a condition, denoted hereafter as CPC, where only the time points where the linear trend profiles of ControllerTS and TemperatureTS have crossed simultaneously opposite thresholds will be marked as incidents. Figure 3 shows an example of the application of CPC on the linear trend profiles of ControllerTS and TemperatureTS on data set DS1.

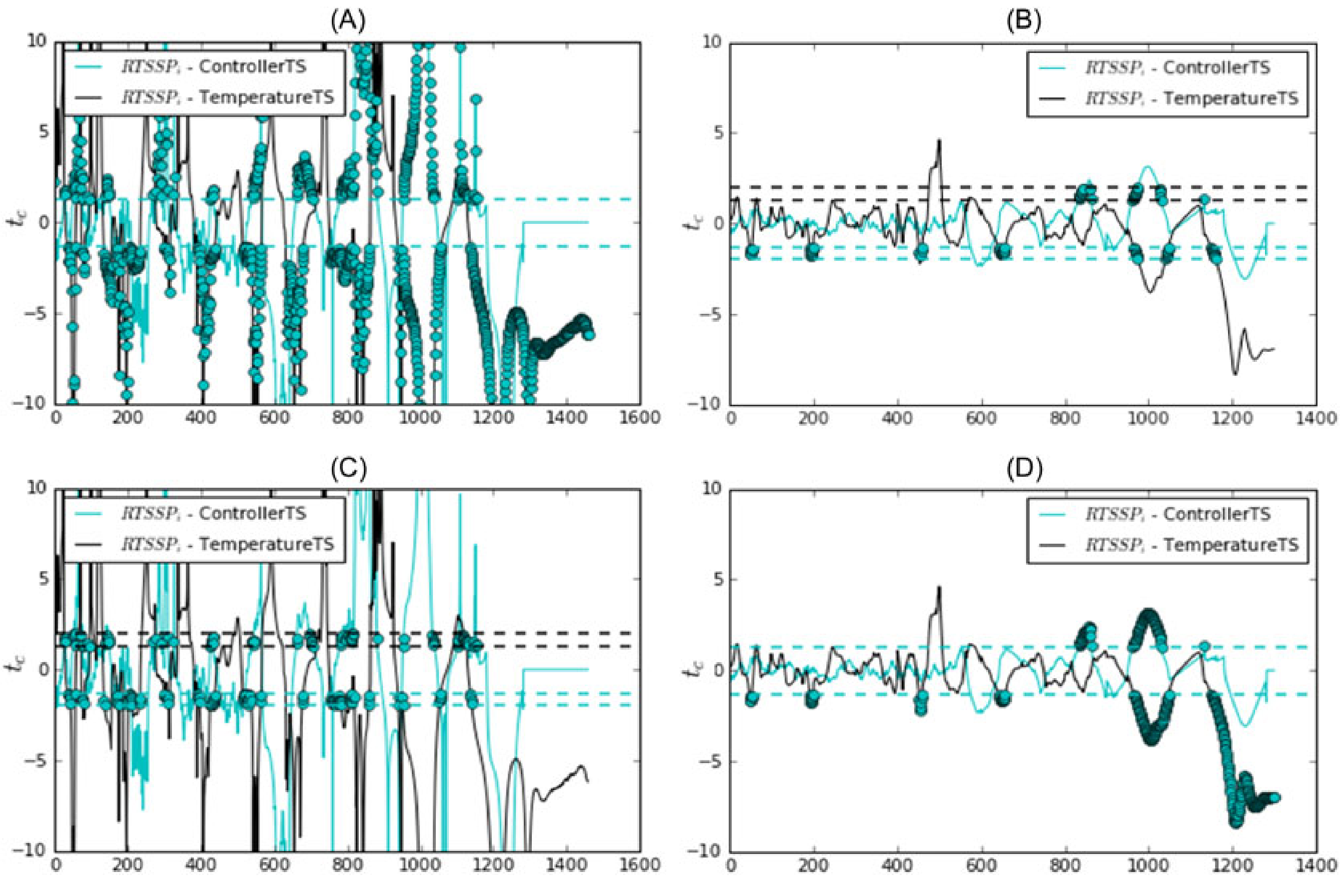

FIGURE 4 Linear trend profiles $\{RTSSP_i\}$ of ControllerTS and TemperatureTS for data set DS1 for all four versions (A) RTSSPv1, (B) RTSSPv2, (C) RTSSPv3, and (D) RTSSPv4 and their possible incidents T. RTSSP, real-time slope statistic profile

It is observed that the application of the CPC on the linear trend profiles of the tested time series has the ability to distinguish the time points that fit the most to the test scenario among all possible incidents T. The application of these additions (self-adaptive sliding window and CPC) to the structure of the RTSSP method has, as a result, increased robustness and effectiveness for the early malfunction diagnosis problem.

5 | COMPARATIVE STUDY

In order to further explore the capabilities of the RTSSP method and have a complete picture about its response, along with versions RTSSPv1 and RTSSPv2, an extended version is proposed (RTSSPv3). At this new variant (RTSSPv3), the computation of the standard error estimator of the trend parameter is $s_1(\hat{\beta})$, and the possible incidents T are detected strictly inside the upper and lower segments. Another version (RTSSPv4) is also considered where the computation of the standard error estimator of the trend parameter is $s_2(\hat{\beta})$, and the possible incidents T are detected when the linear trend profiles of the selected time series cross only UB_1 and LB_1. All the potential combinations of the standard error estimator and cross-checking of thresholds are described below.

Combination 1—standard error estimator: $s_1(\hat{\beta})$ bounds: (LB_1, UB_2) – RTSSPv1
Combination 2—standard error estimator: $s_2(\hat{\beta})$ bounds: (UB_1, UB_2), (LB_1, LB_2) – RTSSPv2
Combination 3—standard error estimator: $s_1(\hat{\beta})$ bounds: (UB_1, UB_2), (LB_1, LB_2) – RTSSPv3
Combination 4—standard error estimator: $s_2(\hat{\beta})$ bounds: (LB_1, UB_2) – RTSSPv4

Figure 4 shows the linear trend profiles of the ControllerTS and TemperatureTS time series, along with the possible incidents T according to all combinations of RTSSP described above, for the DS1 data set. Versions RTSSPv1 (see Figure 4A) and RTSSPv3 (see Figure 4C) provide a higher number of potential incidents T than do versions RTSSPv2 (see Figure 4B)

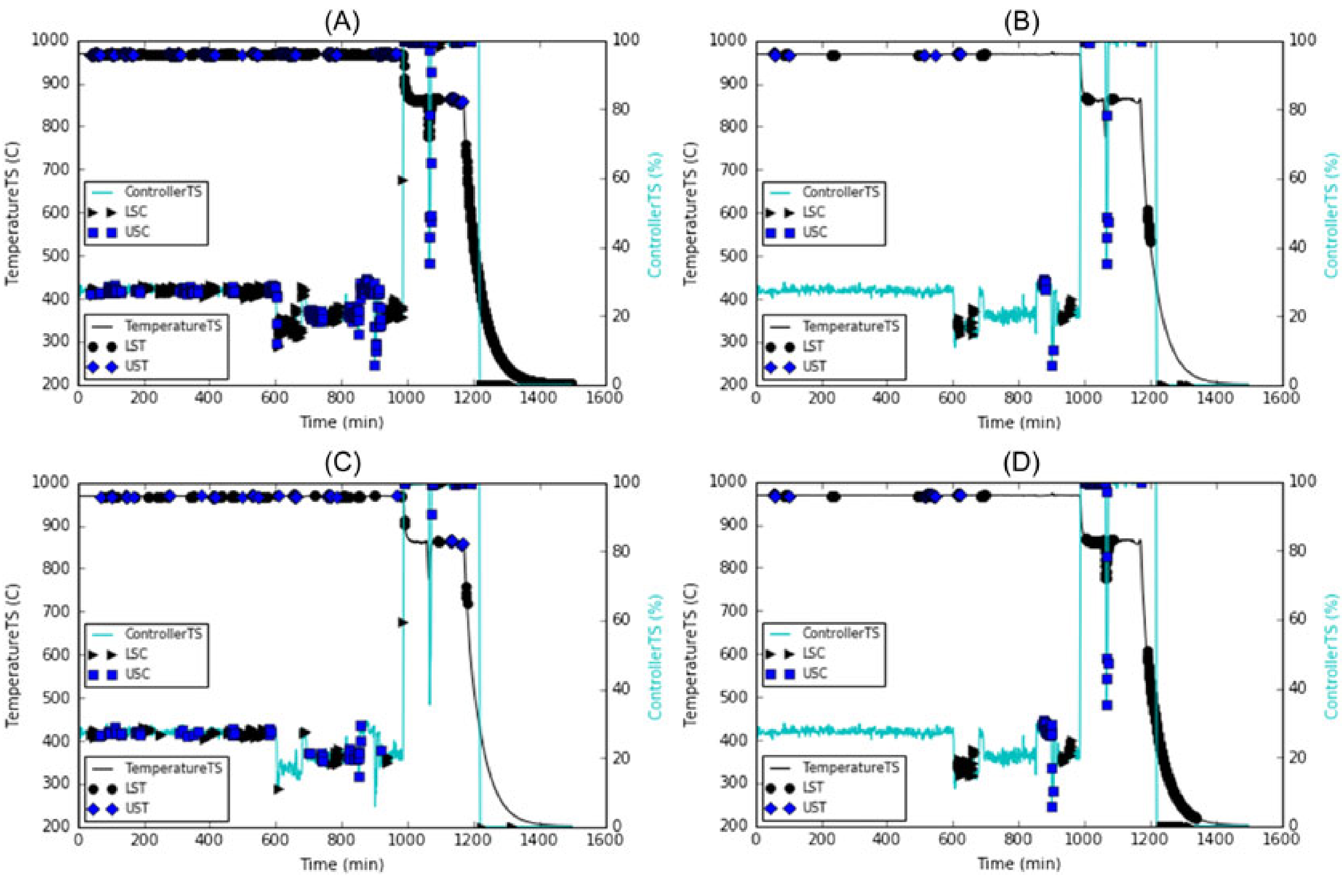

FIGURE 5 Possible incidents T on ControllerTS and TemperatureTS for data set DS1 for all four versions (A) RTSSPv1, (B) RTSSPv2, (C) RTSSPv3, and (D) RTSSPv4. LSC and USC markers denote the lower and the upper segment crossing, respectively, for the controller time series. The same holds for LST and UST for the temperature time series

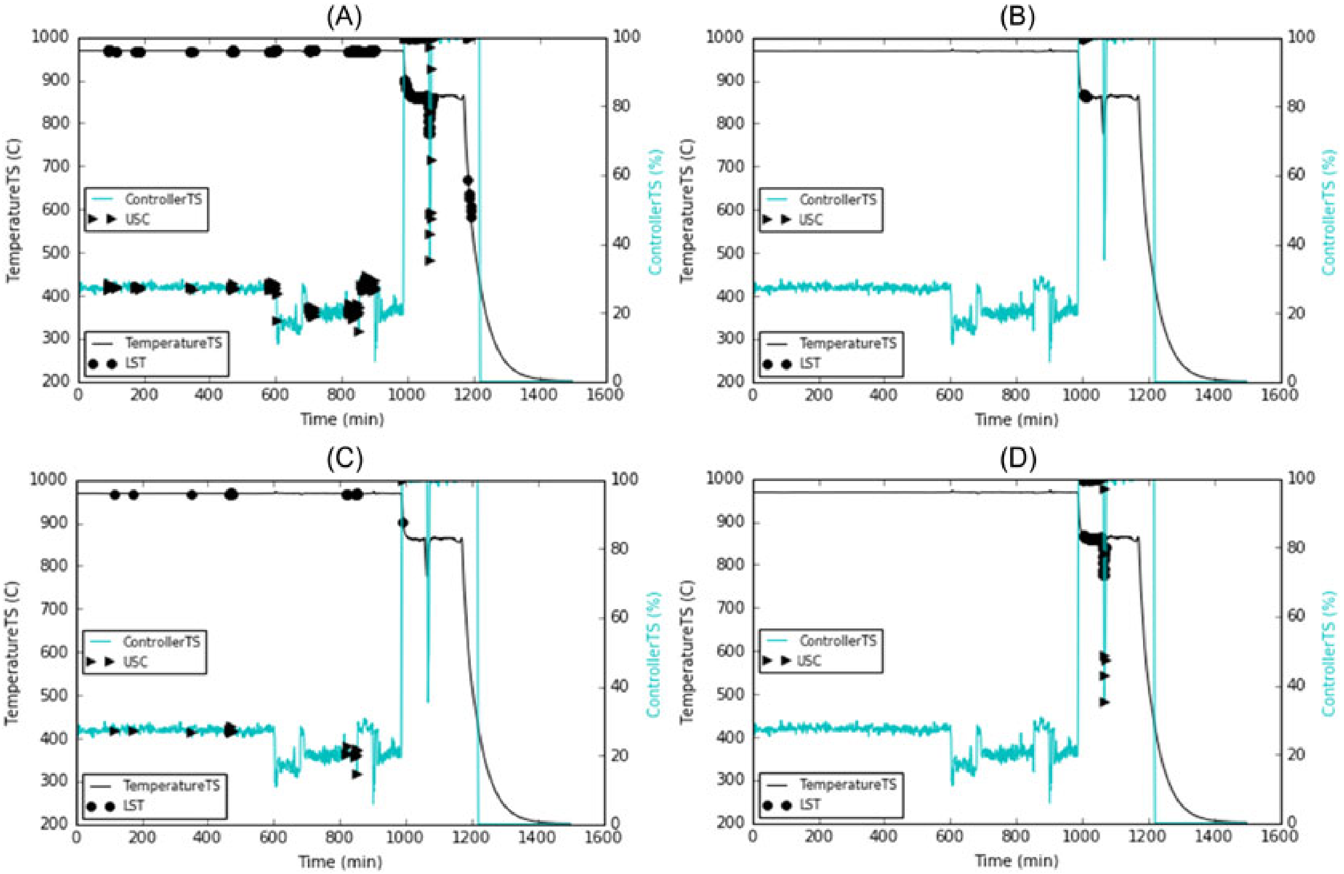

FIGURE 6 Detected incidents T on ControllerTS and TemperatureTS after the application of a common point condition for data set DS1 for all four versions (A) RTSSPv1, (B) RTSSPv2, (C) RTSSPv3, and (D) RTSSPv4. LSC and USC markers denote the lower and the upper segment crossing, respectively, for the controller time series. The same holds for LST and UST for the temperature time series

and RTSSPv4 (see Figure 4D) on the part of the time series before the occurrence of a major incident. This happens because the standard error $s_1(\hat{\beta})$ is more sensitive on the existence of a linear trend than $s_2(\hat{\beta})$.

Figure 5 shows the potential incidents T for all four versions according to the RTSSP method suggestions for DS1, whereas Figure 6 shows the detected incidents T after the application of the CPC for the specified data set. In Figure 5, the potential incidents are the result of the RTSSP crossing in both the upper and lower segments, for the ControllerTS and TemperatureTS time series, which means that the time points where temperature increases and controller decreases are also included. In other words, Figure 5 provides a general view of all linear trend changes (upward and downward) on the tested time series, ControllerTS and TemperatureTS. From Figure 6, it is clear that the application of the CPC is imperative, as it well targets the problem (ControllerTS increases and TemperatureTS decreases). One can see that all versions detect incidents very close to the actual ones, with versions RTSSPv2 (see Figure 6B) and RTSSPv4 (see Figure 6D) to provide very accurate early malfunction diagnosis. On the other hand, version RTSSPv3 (see Figure 6C) provides some detection before the actual one, which could be considered warnings of a future malfunction, whereas version RTSSPv1 (see Figure 6A) indicates a vast number of time points where temperature decreases before the actual malfunction.

Figure 7 shows the linear trend profiles of the ControllerTS and TemperatureTS time series, along with the possible incidents T according to all combinations of the RTSSP described above, for the DS2 data set, whereas Figure 8 shows the potential incidents T for all four versions according to the RTSSP method suggestions for the specified data set. Figure 9 shows the detected incidents T after the application of the CPC for the DS2 data set. The RTSSPv2 (see Figure 9B) and RTSSPv4 (see Figure 9D) versions provide an accurate enough early detection, in terms of time, on TemperatureTS, whereas RTSSPv1 (see Figure 9A) detects incidents more closely (before and after) to the actual malfunction compared to the other versions.

From all of the results described above, it is clear that there is no major difference between versions RTSSPv2 and RTSSPv4, as the detected incidents from RTSSPv4 include those detected from RTSSPv2 while the rest are pointed after them. On the other hand, the issue with RTSSPv1 is the detection of too many time points as incidents compared

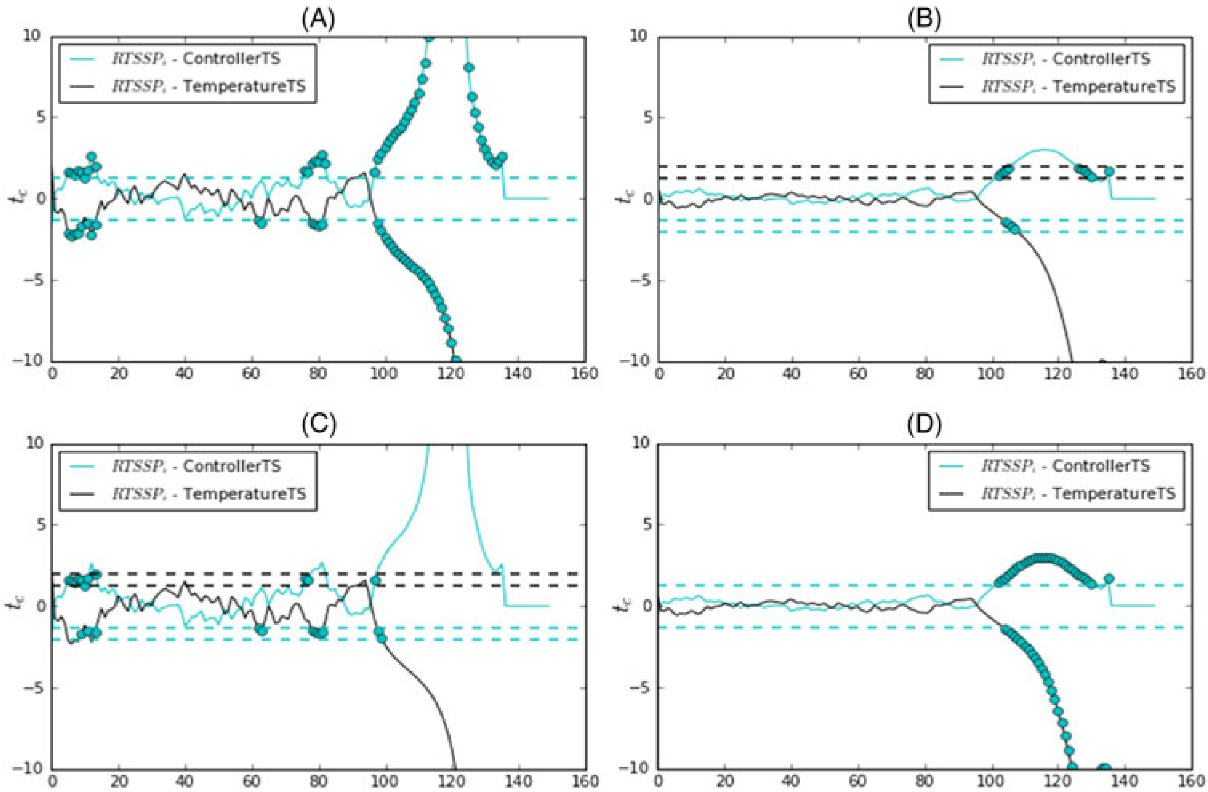

FIGURE 7 Linear trend profiles $\{RTSSP_i\}$ of ControllerTS and TemperatureTS for data set DS2 for all four versions (A) RTSSPv1, (B) RTSSPv2, (C) RTSSPv3, and (D) RTSSPv4 and their possible incidents T. RTSSP, real-time slope statistic profile

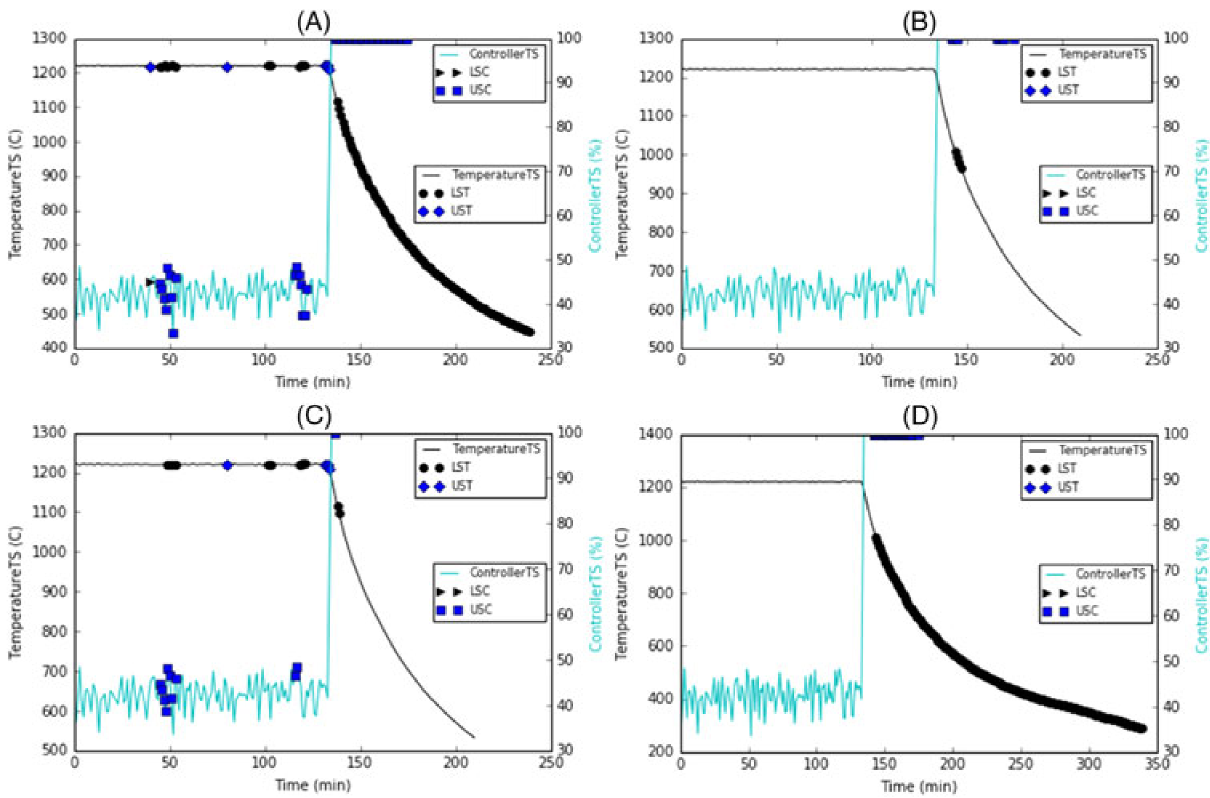

FIGURE 8 Possible incidents T on ControllerTS and TemperatureTS for data set DS2 for all four versions (A) RTSSPv1, (B) RTSSPv2, (C) RTSSPv3, and (D) RTSSPv4. LSC and USC markers denote the lower and the upper segment crossing, respectively, for the controller time series. The same holds for LST and UST for the temperature time series

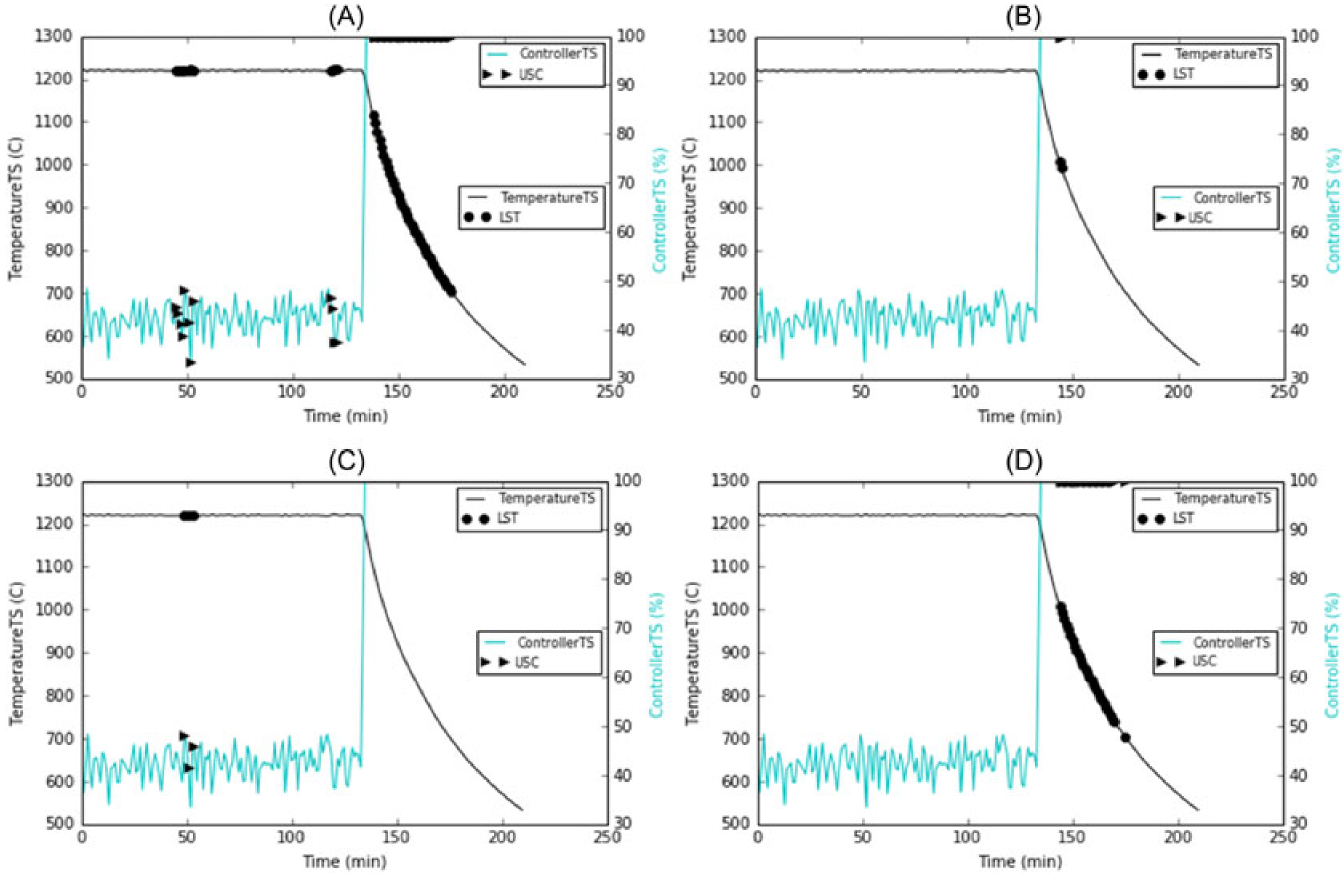

FIGURE 9 Detected incidents T on ControllerTS and TemperatureTS after the application of a common point condition for data set DS2 for all four versions (A) RTSSPv1, (B) RTSSPv2, (C) RTSSPv3, and (D) RTSSPv4. LSC and USC markers denote the lower and the upper segment crossing, respectively, for the controller time series. The same holds for LST and UST for the temperature time series

to RTSSPv3, but it has the benefit that at all tested cases, it can provide some incident detection closer to the actual malfunction compared to RTSSPv3.

To summarize, versions RTSSPv2 and RTSSPv4 are very reliable and have adequate accuracy in their response in order to provide diagnosis notification in case of temperature dropping. On the other hand, versions RTSSPv1 and RTSSPv3 can also provide accurate early malfunction diagnosis, especially version RTSSPv1, but both are more sensitive on linear trend variations, a fact that has, as a result, these variations to be pointed as incidents. This is not necessarily a negative fact because these small variations in the linear trend can be forerunners that a malfunction is to be held in the near future. Thus, depending on the criticality of the area, which is observed, or the criticality of the experiment, the process operator or process engineer can opt to have either many notifications with an increased potential of false warnings or a more ridged method such that only the incidents with high potential will appear.

6 | CONCLUSIONS

Generally, the use of linear trend analysis with real-time classification provides a robust signal processing technique on the real-time incident detection problem. These aforementioned scientific fields and techniques synergistically coexist in the method of RTSSP. The use case scenario for early malfunction diagnosis that is tested focuses on the detection of the time point where the temperature time series drops along with the simultaneous detection of the increase of the controller time series (temperature and controller time series are inversely proportional). The comparative analysis between the four versions of the RTSSP method has distinguished two of them as the most appropriate for the use case scenario. The most suitable versions for the specified incident detection problem are RTSSPv1 (standard error estimator $s_1(\hat{\beta})$ with bounds at (LB_1, UB_2)) and RTSSPv2 (standard error estimator $s_2(\hat{\beta})$ with double bounds at (UB_1, UB_2), (LB_1, LB_2)). The choice between these two versions of the RTSSP method, along with the selection of core parameter values, can be done by the end user according to the needs and the nature of the problem.

The method of RTSSP can be easily modified and adapted to three other potential use cases: (1) both temperature and controller time series decrease (shutdown state), (2) both temperature and controller time series increase (startup or condition change state), and (3) temperature time series increases and controller time series decreases (reaction state). The RTSSP method is also tested on these use cases with some very good preliminary results. As a future extension of this work, a generalized version including these cases will be considered as extra scenarios for the detection of specific operating states of the chemical process.

ACKNOWLEDGEMENT

This work was partially supported by the European Commission through the Horizon 2020 Framework Programme, Innovation Actions (IA), and the SatisFactory project through Grant 636302.

ORCID

T. Vafeiadis http://orcid.org/0000-0003-3682-7539

REFERENCES

1. Papadopoulos S, Drosou A, Dimitriou N, Abdelrahman OH, Gorbil G, Tzovaras D. A BRPCA based approach for anomaly detection in mobile networks. In: Abdelrahman OH, Gelenbe E, Gorbil G, Lent R, eds. *Information Sciences and Systems 2015: 30th International Symposium on Computer and Information Sciences (ISCIS 2015).* Cham, Switzerland: Springer International Publishing Switzerland; 2015:115-125.
2. Markou M, Singh S. Novelty detection: a review—part 2: neural network based approaches. *Signal Process*. 2003;83(12):2499-2521.
3. Abdulhai B, Ritchie SG. Enhancing the universality and transferability of freeway incident detection using a Bayesian-based neural network. *Transp Res C Emerg Technol*. 1999;7(5):261-280.
4. Yuan F, Cheu RL. Incident detection using support vector machines. *Transp Res C Emerg Technol*. 2003;11(3):309-328.
5. Wang J, Li X, Liao SS, Hua Z. A hybrid approach for automatic incident detection. *IEEE Trans Intell Transp Syst*. 2013;14(3):1176-1185.
6. Thiprungsri S, Vasarhelyi MA. Cluster analysis for anomaly detection in accounting data: an audit approach. *Int J Digit Account Res*. 2011;11:69-84.
7. Vafeiadis T, Bora-Senta E, Kugiumtzis D. Estimation of linear trend onset in time series. *Simul Model Pract Theory*. 2011;19(5):1384-1398.
8. Markou M, Singh S. Novelty detection: a review—part 1: statistical approaches. *Signal Process*. 2003;83(12):2481-2497.
9. Weil R, Wootton J, García-Ortiz A. Traffic incident detection: sensors and algorithms. *Math Comput Model*. 1998;27(9-11):257-291.
10. Feidas H, Makrogiannis T, Bora-Senta E. Trend analysis of air temperature time series data in Greece determined by ground and satellite data. *Theor Appl Climatol*. 2004;79:185-208.
11. Gil-Alana LA. Time trend estimation with breaks in temperature time series. *Clim Change*. 2008;89(3-4):325-337.
12. Iglesias F, Zseby T. Analysis of network traffic features for anomaly detection. *Mach Learn*. 2015;101(1-3):59-84.
13. Papadopoulos S, Drosou A, Tzovaras D. A novel graph-based description for the detection of billing-related anomalies in cellular mobile networks. *IEEE Trans Mob Comput*. 2016;15(11):2655-2668.
14. Perron P, Zhu X. Structural breaks with deterministic and stochastic trends. *J Econ*. 2005;129(1-2):65-119.
15. Zivot E, Andrews DWK. Further evidence on the great crash, the oil price shock, and the unit root hypothesis. *J Bus Econ Stat*. 1992;10(3):251-270.
16. Zheng Y, Rajasegarar S, Leckie C, Palaniswami M. Smart car parking: temporal clustering and anomaly detection in urban car parking. In: Proceedings of the IEEE Ninth International Conference on Intelligent Sensors, Sensor Networks and Information Processing (IEEE ISSNIP); 2014; Piscataway, NJ.
17. Botre C, Mansouri M, Nounou M, Nounou H, Nazmul Karim M. Kernel PLS-based GLRT method for fault detection of chemical processes. *J Loss Prev Process Ind*. 2016;43:212-224.
18. Bai J, Perron P. Estimating and testing linear models with multiple structural changes. *Econometrica*. 1998;66:47-78.
19. Bai J, Perron P. Computation and analysis of multiple structural change models. *J Appl Econ*. 2003;18:1-22.
20. Subramaniam S. Literature review of incident detection algorithms to initiative diversion strategies [working paper]. Blacksburg, VA: University Center of Transportation Research, Virginia Polytechnic Institute and State University; 1991.
21. Stephanedes YJ, Chassiakos AP, Michalopoulos PG. Comparative performance evaluation of incident detection algorithms. *Transp Res Rec*. 1992;1360:50-57.
22. Balke KN. An evaluation of existing incident detection algorithms. Research Report, FHWA/TX-93/1232-20. College Station, TX: Texas Transportation Institute, The Texas A&M University System; 1993.

23. Mahmassani HS, Haas C, Zhou S, Peterman J. Evaluation of incident detection methodologies. Research Report, 1795-1. Austin, TX: Center for Transportation Research, The University of Texas at Austin; 1999.
24. Peterman J. *Calibration and Evaluation of Automatic Incident Detection Algorithms* [master's thesis]. Austin, TX; University of Texas; 1999.
25. Black J, Sreedevi I. Automatic incident detection algorithms. Berkeley, CA: ITS Decision Database in PATH; 2001.
26. Venkatasubramanian V, Rengaswamy R, Yin K, Kavuri SN. A review of process fault detection and diagnosis: part I: quantitative model-based methods. *Comput Chem Eng*. 2003;27(3):293-311.
27. Vafeiadis T, Bora-Senta E, Kugiumtzis D. Evaluation of linear trend tests using resampling techniques. *Commun Stat Simul Comput*. 2008;37(5):907-923.
28. Vafeiadis T, Krinidis S, Ziogou C, Ioannidis D, Voutetakis S, Tzovaras D. Robust malfunction diagnosis in process industry time series. Paper presented at: 2016 IEEE 14th International Conference of Industrial Informatics (INDIN); 2016; Poitiers, France.
29. Vafeiadis T, Ioannidis D, Krinidis S, Ziogou C, Voutetakis S, Tzovaras D, Likothanassis S. Real-time incident detection: an approach for two interdependent time series. Paper presented at: 2016 24th European Signal Processing Conference (EUSIPCO); 2016; Budapest, Hungary.
30. Woodward WA, Gray HL. Global warming and the problem of testing for trend in time series data. *J Climate*. 1993;6(5):953-962.

How to cite this article: Vafeiadis T, Ziogou C, Stavropoulos G, et al. Early malfunction diagnosis of industrial process units utilizing online linear trend profiles and real-time classification. *Int J Adapt Control Signal Process*. 2018;1–13. https://doi.org/10.1002/acs.2915